Single-channel 15.3 Tbit/s, 64 QAM coherent Nyquist pulse transmission over 150 km with a spectral efficiency of 8.3 bit/s/Hz

doi: 10.1364/OE.27.028952

Research Article | Vol. 27, No. 20 / 30 September 2019 / Optics Express 28952
Optics EXPRESS

Single-channel 15.3 Tbit/s, 64 QAM coherent Nyquist pulse transmission over 150 km with a spectral efficiency of 8.3 bit/s/Hz

MASATO YOSHIDA,* KOSUKE KIMURA, TARO IWAYA, KEISUKE KASAI, TOSHIHIKO HIROOKA, AND MASATAKA NAKAZAWA

Research Institute of Electrical Communication, Tohoku University, 2-1-1 Katahira, Aoba-ku, Sendai, 980-8577, Japan
*masato@riec.tohoku.ac.jp

Abstract: We report the first single-channel 15.3 Tbit/s, 1.28 Tbaud, 64 QAM transmission using 670 fs coherent Nyquist pulses. We newly constructed an optical gate to improve the signal-to-noise ratio (SNR) of the homodyne detection signal, a coherent spectral expansion technique, and an optical phase-locked loop (OPLL) circuit with a 0.6 deg. phase noise. We also constructed an active 70 fs timing stabilization circuit between the OTDM signal and Nyquist LO pulse to realize precise homodyne detection. With these new techniques, we successfully achieved a record speed of 15.3 Tbit/s in a single channel transmission over 150 km with a spectral efficiency of 8.3 bit/s/Hz.

1. Introduction

Information traffic has been rapidly growing with the spread of broadband services such as ultra-high definition video delivery, fifth-generation mobile communications (5G), and the use of big data analyses. To satisfy these traffic demands, finding a way to realize faster network interfaces with a single-channel bit rate exceeding 1 Tbit/s and a higher spectral efficiency (SE) have become important research subjects. To realize symbol rates exceeding 100 Gbaud, high-speed optical and electronic devices have widely developed. For example, 192 Gbaud, quadrature phase shift keying (QPSK) signal generation with an InP-based IQ modulator [1] and 100 Gbaud, 32 quadrature amplitude modulation (QAM) signal generation with an all-silicon IQ modulator [2] have been demonstrated, which have enabled the use of a single-channel bit rate of around 1 Tbit/s.

On the other hand, optical time division multiplexing (OTDM) transmission with a coherent Nyquist pulse is also an attractive method for simultaneously achieving a single-channel transmission beyond Tbit/s and a high SE [3–5]. In this scheme, coherent pulse detection with the Nyquist LO pulse enables demultiplexing and homodyne detection simultaneously [6], resulting in no need for a TDM demultiplexer. This greatly simplified the system. In our previous work, we reported a single-channel 7.68 Tbit/s, 64 QAM coherent Nyquist pulse transmission over 150 km with an SE of 9.7 bit/s/Hz [5]. However, the signal level for the demodulated tributary became lower when the goal was a higher baud rate transmission, which degraded the signal-to-noise ratio (SNR). To further increase the baud rate, it is important to improve the SNR of the homodyne-detection signal.

In this paper, we demonstrate the first single-channel 15.3 Tbit/s, 1.28 Tbaud, 64 QAM-150 km transmission by adopting an optical gate, spectral expansion with high coherency for the generation of ultra-short coherent pulses, an ultrastable optical phase-locked loop (OPLL) technique with a 0.6 deg. phase noise and a 70 fs timing stabilization circuit between the OTDM signal and the LO pulse. A $LiNbO_3$ modulator was used as an optical gate, where part of the OTDM signal at around the target tributary is allowed to pass, and the other tributaries are removed prior to

#375329 https://doi.org/10.1364/OE.27.028952
Journal © 2019 Received 13 Aug 2019; revised 10 Sep 2019; accepted 11 Sep 2019; published 25 Sep 2019

Optics EXPRESS

homodyne detection. With this optical gate, the bit error rate (BER) for a back-to-back condition was improved by approximately one order of magnitude. A 7 m-long highly nonlinear fiber (HNLF) was used to expand the spectral profile without coherence degradation [7]. We also reduced the phase noise in the OPLL circuit to as small as 0.6 deg. by shortening the loop length to approximately 18 m. Furthermore, we constructed an active stabilization circuit for the timing between the OTDM signal and Nyquist LO pulse to realize stable long-term homodyne detection. The timing drift was reduced to less than 70 fs. With these improvements, we successfully obtained BERs below a 25.5% forward error correction (FEC) limit of 3.8×10^{-2} for all 128 tributaries of the OTDM signal after a 150 km transmission. Thus, we achieved a record speed of 15.3 Tbit/s in a single-channel transmission with an SE of 8.3 bit/s/Hz.

2. Experimental setup for single-channel 15.3 Tbit/s, 64 QAM coherent Nyquist pulse transmission over 150 km

Figure 1 shows our experimental setup for a single-channel 15.3 Tbit/s coherent Nyquist pulse transmission over 150 km. In this system, we set the symbol rate of the baseline signal at 9.953 Gbaud, but for the sake of simplicity we describe it as 10 Gbaud. Compared with our previous work on 7.68 Tbit/s transmission [5], a doubled bandwidth and more precise handling of the shorter Nyquist pulse are required. This section describes new techniques for realizing a 15.3 Tbit/s transmission.

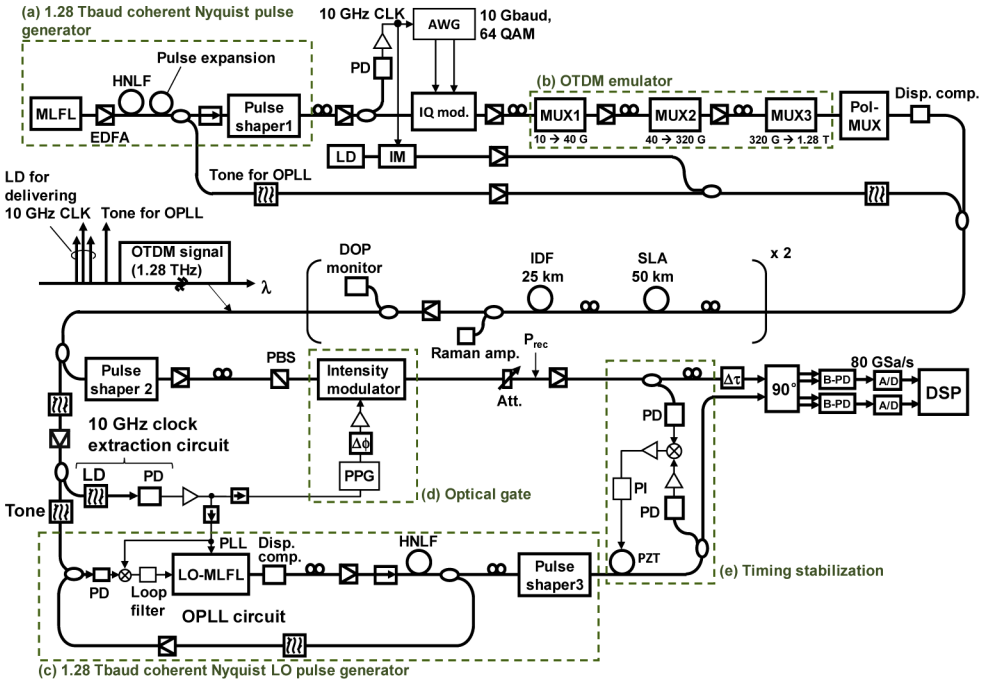

Fig. 1. Experimental setup for a single-channel 15.3 Tbit/s -150 km 64 QAM coherent Nyquist pulse transmission.

2.1. 15.3 Tbit/s coherent Nyquist pulse transmitter

We used a mode-hop-free, picosecond 10 GHz mode-locked pulse fiber laser (MLFL) as a transmitter [8–10]. To generate an ultrafast Nyquist pulse train for a 1.28 Tbaud transmission, the laser output spectrum was broadened to 11.5 nm at a bandwidth of 6 dB by using a 7 m-long

Optics EXPRESS

HNLF with a normal dispersion of - 0.6 ps/nm/km. The launch power was 24 dBm. To prevent coherence degradation in the spectral broadening process [7], we reduced the length of the HNLF from 20 m to 7 m. After the spectral broadening, the signal was shaped into an optical Nyquist pulse train by using pulse shaper 1, which is a liquid crystal on silicon device (see dashed-line box (a) in Fig. 1). The filtering sharpness of the pulse shaper was -190 dB/nm. The obtained Nyquist pulse was then 64 QAM-modulated at 10 Gbaud. The 64 QAM signal was multiplexed up to 1.28 Tbaud with an OTDM emulator composed of three OTDM multiplexers (10 G→40 G, 40 G→320 G, and 320 G→1280 G), which had insertion losses of 6.0, 11.5 and 8.5 dB, respectively. These losses were compensated for with erbium-doped fiber amplifiers (EDFAs) (see dashed-line box (b) in Fig. 1). Here, to suppress the nonlinear phase rotation induced in these EDFAs, we employed a second-order dispersion of - 3.0 ps/nm and expanded the input pulse width to approximately 26 ps in front of the pulse shaper 1 [5]. The spectral profile remained unchanged after the pulse expansion. The expanded pulse was passed through the transmitter by keeping the pulse width at more than 20 ps. Then, the chirping that accompanied the pulse expansion was compensated for with a dispersion compensator after OTDM and polarization multiplexing. As a result, a transform-limited Nyquist pulse train was obtained in front of a 150 km transmission line.

At the transmitter, the 72nd harmonic signal of the broadened spectrum was extracted with an optical narrow filter and used as a pilot tone for the optical phase-locking of the Nyquist LO pulse. Furthermore, an intensity modulated laser diode (LD) signal was used to deliver a 10 GHz clock. In our previous work [5], we extracted the clock signal from the OTDM signal by using an electro-optical PLL circuit with an electro-absorption modulator (EAM) [11]. Although this circuit was designed for OTDM signals with constant amplitude modulation formats such as on-off keying (OOK), binary phase shift keying (BPSK) and QPSK, a small timing fluctuation of 0.5 ps was randomly induced in the output clock signal. This fluctuation is nonnegligible for a 1.28 Tbaud transmission. Therefore, we newly prepared an LD as shown in Fig. 1 for the clock delivery with a timing jitter of less than 110 fs. The pilot tone and LD signals were combined with the OTDM data, and these signals were launched into a 150 km transmission line.

The optical spectrum and waveform of the MLFL output are shown in Figs. 2(a) and 2(b), respectively. The center wavelength, spectral width, and pulse width of the laser output were 1544 nm, 2.3 nm (285 GHz), and 1.55 ps, respectively. The time-bandwidth product was 0.44, indicating that the output pulse was a transform-limited Gaussian pulse. Figure 2(c) shows the optical spectrum obtained after spectral expansion using a 7 m-long HNLF. The 6 dB-spectral width was 11.3 nm, which is sufficiently large to generate a Nyquist pulse for 1.28 Tbaud transmission.

Figure 3 shows the pulse characteristics measured in front of a 150 km transmission line. Since the IQ modulator and the OTDM emulator may induce changes in the spectrum, we replaced these devices with optical attenuators in the precise pulse measurement. Figures 3(a-1) and 3(a-2) show the optical spectra of generated Nyquist pulse signals with roll-off factors $\alpha = 0$ and 0.1, respectively. The obtained spectra agree well with the ideal Nyquist pulse spectra shown by the red curves. In Fig. 3(a-1), residual components with a power level of -15 dB were observed in both spectral edges due to the finite sharpness (-190 dB/nm) of the pulse shaper. The corresponding autocorrelation waveforms are shown in Figs. 3(b-1) and 3(b-2), respectively. As a reference, the red dashed and solid curves show the ideal Nyquist pulse waveform and its autocorrelation waveform, respectively. The measured waveforms accurately fit the ideal autocorrelation waveforms. From the autocorrelation measurement, the FWHMs of both the generated Nyquist pulses are estimated to be 670 fs.

In our experiment, we were able to generate a Nyquist pulse with an arbitrary roll-off factor. By reducing the spectral width of the Nyquist pulse with a lower α value, we can improve the SE. However, the ringing in the tail of an $\alpha = 0$ Nyquist pulse oscillates over a longer time, resulting

Optics EXPRESS

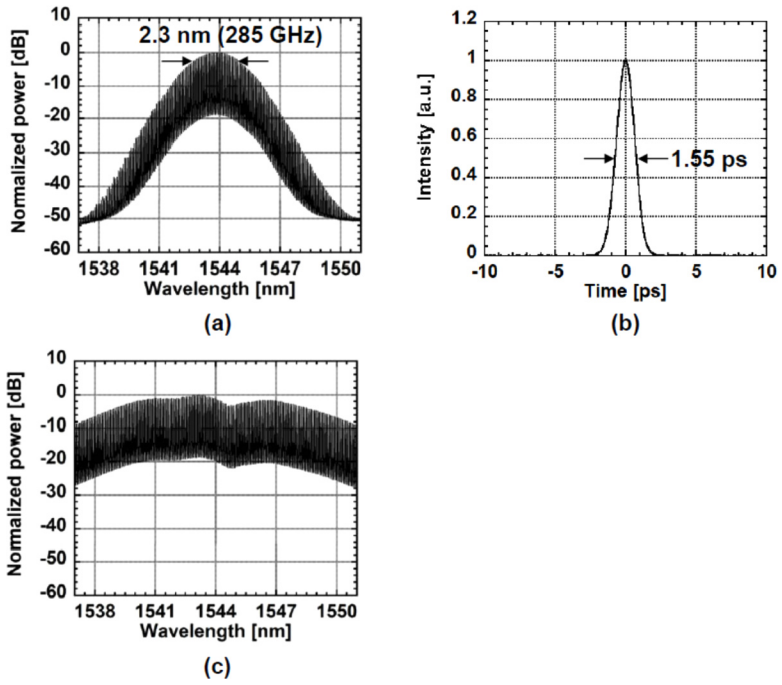

Fig. 2. (a) Optical spectrum and (b) waveform of a 10 GHz MLFL output pulse. (c) is the optical spectrum obtained after spectral expansion with an HNLF.

a larger inter-symbol interference (ISI) from other time slots since we used homodyne detection with a Nyquist LO pulse for the OTDM demultiplexing instead of the optical sampling method. Therefore, a Nyquist pulse train with $\alpha \neq 0$ is preferable. However, when we use such a Nyquist pulse, the time-domain orthogonality of the pulse is degraded [6]. By considering these tradeoff relations, we set α at 0.1.

Figure 4 shows the waveform of a generated 640 Gbaud, 64 QAM Nyquist OTDM signal using an optical sampling oscilloscope with a 500 fs resolution. It can be seen that the intensity of each tributary pulse is approximately equal to a 1.57 ps separation. Here, it was difficult to clearly observe an OTDM signal with a higher baud rate due to the oscilloscope resolution.

2.2. 150 km transmission line

The transmission line we used consisted of two 75 km spans with a 50 km super large area fiber (SLA, dispersion: 20 ps/nm/km, dispersion slope: 0.07 ps/nm^2/km) and a 25 km inverse dispersion fiber (IDF, dispersion: - 40 ps/nm/km, dispersion slope: - 0.14 ps/nm^2/km) so that the second- and third-order dispersions were compensated for simultaneously. The average loss was 16.8 dB/span, which was compensated for by the combination of a Raman amplifier (10 dB gain) and an EDFA (6.8 dB gain). The gain flatness of the in-line EDFA and Raman amplifiers was less than 1 dB. Two polarization controllers (PCs) were installed in each span to mitigate the first-order polarization-mode dispersion (PMD) of the transmission line. The PCs were adjusted to realize the maximum degree of polarization (DOP) of the signal after a 150 km transmission. The PMDs of the SLA and IDF were relatively large at 0.02 ps/km$^{1/2}$ and 0.04 ps/km$^{1/2}$, respectively. Therefore, it was important to precisely adjust the signal polarization to the principal state of polarization of each fiber with each PC, which enabled us to obtain a DOP of nearly 1.0. In the present system, all the PCs were adjusted manually since the state of polarization was not rapidly changed. The residual second- and third-order dispersions were

Optics EXPRESS

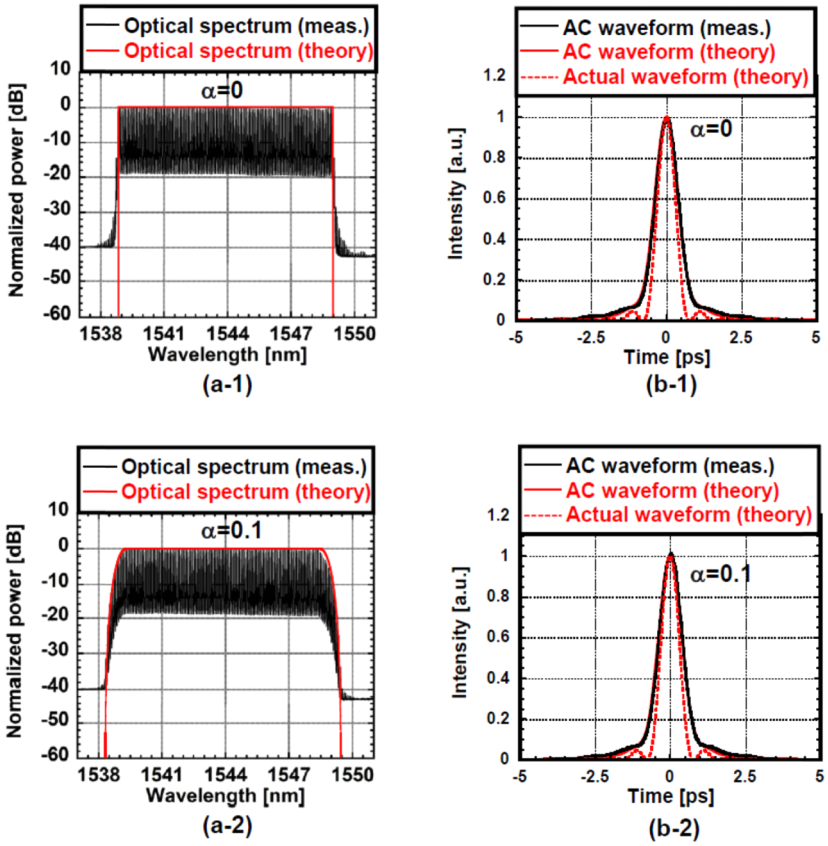

Fig. 3. (a-1) and (a-2) Optical spectra and (b-1) and (b-2) autocorrelation waveforms of generated Nyquist pulses with $\alpha = 0$ and 0.1, respectively.

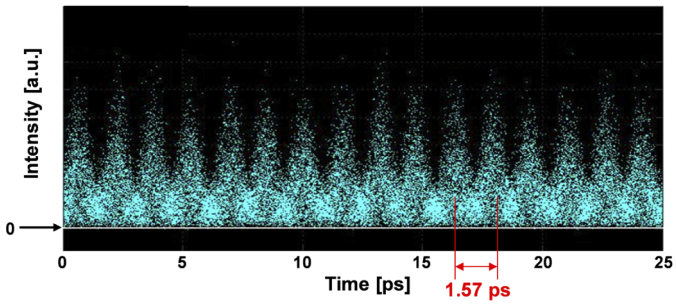

Fig. 4. Waveform of a 64 QAM-OTDM signal at 640 Gbaud.

Optics EXPRESS

precisely compensated for by pulse shaper 2 with accuracies of $|\beta_2 L| < 0.01$ ps^2 and $|\beta_3 L| < 0.01$ ps^3, respectively. In pulse shaper 2, the spectral profile was also re-shaped simultaneously.

Figures 5(a) and 5(b) show the optical spectra of a 15.3 Tbit/s OTDM signal before and after a 150 km transmission, respectively. The launched power was 5 dBm. In our OTDM emulator, the same 10 Gbaud data were interleaved with a fixed time delay. Therefore, neighboring tributaries interfered and generated spectral fringes. The left figure in Fig. 5(a) shows an enlarged view around the pilot tone and intensity modulated LD signals. The bandwidth of these signals was approximately 60 GHz, which is negligible compared with that for the OTDM signal of 1.41 THz. Since it is difficult to define the OSNR of an OTDM signal with such a spectral fringe, we estimated it under a baseline transmission condition, where the OTDM multiplexers were replaced by optical attenuators with an identical loss. Thus, the estimated OSNRs for one tributary channel before and after a 150 km transmission were 35.0 and 21.5 dB, respectively.

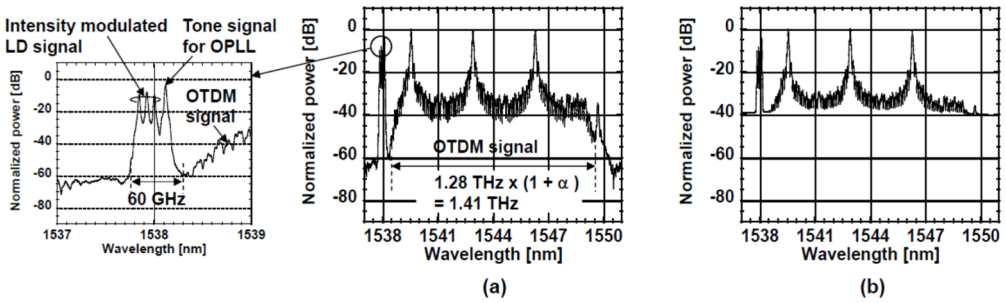

Fig. 5. Optical spectra of 15.3 Tbit/s OTDM signal. (a) before transmission, (b) after 150 km transmission.

To evaluate the polarization crosstalk due to the second-order PMD (depolarization) during a 150 km fiber transmission, we measured the optical spectrum of one polarization channel and that of the leaked component to the other polarization channel. Figure 6 shows the result, where red and blue curves correspond to the signal and crosstalk components, respectively. The crosstalk estimated from the integrated spectrum power ratio was - 23 dB. When we installed only one PC in each span, the crosstalk increased to - 20 dB. This indicates that precise polarization control is very important for an ultrahigh baud rate transmission with a spectral width of more than 10 nm.

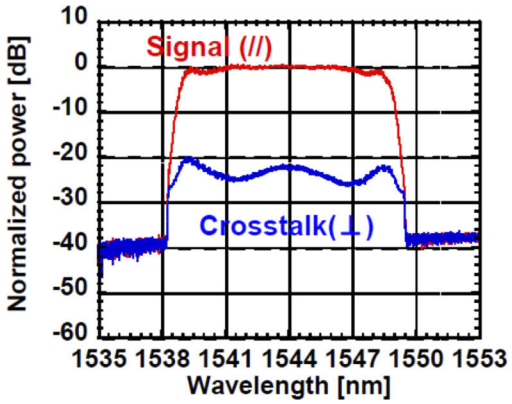

Fig. 6. Optical spectra of signal and crosstalk after 150 km propagation.

Optics EXPRESS

2.3. Generation of coherent Nyquist LO pulse train

At the receiver, part of the transmitted signal was coupled to a clock extraction circuit consisting of an optical filter and a photodiode (PD), where a 10 GHz clock signal was extracted from an intensity modulated LD signal. Figures 7(a) and 7(b) show the RF spectrum and the single side band (SSB) noise spectrum of the 10 GHz clock signal. By integrating the SSB phase noise from 100 Hz to 10 MHz, the timing jitter was estimated to be 0.11 ps, which is sufficiently small for the present experiment. The clock signal was used to control the repetition rate and the optical phase of the Nyquist LO pulse [5]. Here, the LO pulse source was composed of an MLFL and a 7 m-long HNLF. In the OPLL circuit, the error signal between the clock signal and a beat signal, which was generated by the pilot tone and the 71st harmonics of the LO spectrum, was fed back to the LO-MLFL (see dashed-line box (c) in Fig. 1).

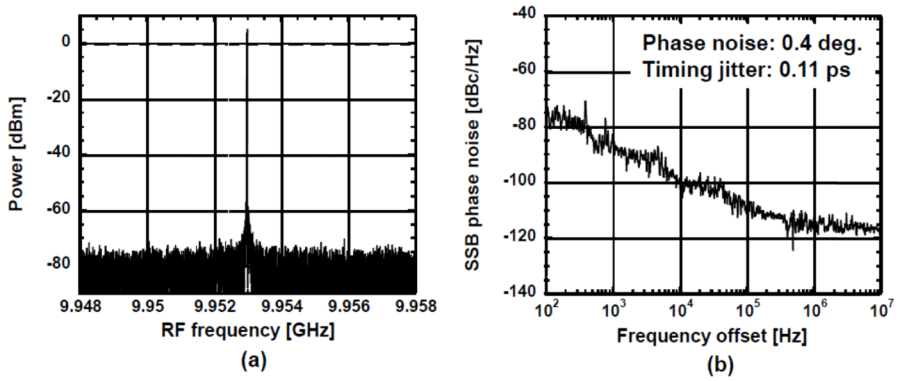

Fig. 7. (a) RF spectrum and (b) SSB phase noise of a 10 GHz clock signal extracted from an intensity modulated LD signal after a 150 km transmission.

The optical spectrum and waveform of the LO-MLFL output are shown in Figs. 8(a) and 8(b), respectively. The spectral width and pulse width of the laser output pulse were 2.2 nm (270 GHz) and 2.0 ps, respectively. Compared with the MLFL at the transmitter, the LO-MLFL was equipped with an etalon filter with a lower Q value, resulting in a wide tunable range as regards the repetition rate and the optical frequency of the laser output [10]. The tunability is important if we are to lock the repetition rate and optical phase of the LO-MLFL to those of the OTDM signal. Since the free spectral range (FSR) of the etalon with a low finesse was not exactly equal to the repetition rate, the spectral bandwidth of the LO-MLFL was relatively narrow compared with that of the transmitter (see Fig. 2(a)). Figure 8(c) shows the optical spectrum after spectral broadening. A 10 nm bandwidth was obtained at - 14 dB down from the signal peak, which means a shaping loss of 16 dB in pulse shaper 3. However, the shaping loss was allowable because the required optical power for the Nyquist LO pulse was only 2 dBm with our balanced PD. Figure 9 shows the optical spectra and autocorrelation waveforms of the generated Nyquist LO pulse signals with roll-off factors $\alpha = 0$ and 0.1, respectively. Thus, we could prepare Nyquist LO pulses with as high a shaping accuracy as those generated at the transmitter.

Figure 10 shows the RF spectrum and the single side band (SSB) noise spectrum of the IF signal in the OPLL circuit, where it is important to shorten the loop length to obtain a wider controlling bandwidth. Therefore, we shortened the length of the HNLF to 7 m and increased the launched power to 27 dBm with a high power EDFA. We constructed the EDFA using a 2 m-long EDF with a high Er ion concentration (3500 ppm). As a result, the total loop length became 18 m and we obtained a phase noise of as small as 0.6 deg. as shown in Fig. 10(b). The phase noise is sufficiently small for 64 QAM demodulation.

Optics EXPRESS

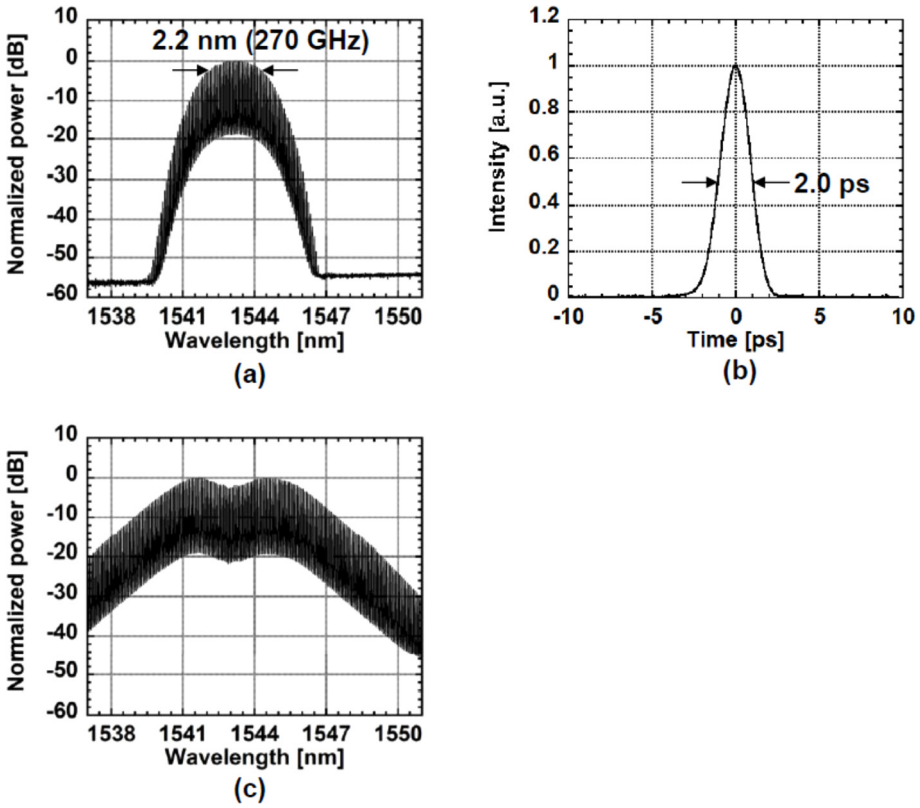

Fig. 8. (a) Optical spectrum and (b) waveform of a 10 GHz LO-MLFL output pulse. (c) is the optical spectrum after spectral broadening with an HNLF.

2.4. Optical gate to increase SNR

After the transmission, the OTDM signal was separated into two orthogonal polarization channels with a polarization-beam splitter (PBS). Then, one of the signals was coupled to an optical gate with a $LiNbO_3$ intensity modulator driven by a "10001000. . . " pattern from a 40 Gbit/s pulse pattern generator (see dashed-line box (d) in Fig. 1). With this gate, only the OTDM data near the test tributary can be extracted. Then, the gated OTDM data were homodyne-detected with the phase-locked Nyquist LO pulse, where we used the time-domain orthogonality of the Nyquist pulse [6]. Finally, the detected data were A/D-converted and demodulated offline with a digital signal processor (DSP). We used 89600 VSA software as the DSP, which includes a finite impulse filter with 99 taps, carrier frequency recovery, and symbol clock recovery. Without this gate operation, it is difficult to obtain a high SNR signal since the average power input into a balanced PD is limited. It also induces residual self-beat noise from the OTDM signal. This problem becomes more serious in a higher baud rate transmission. By increasing the gating effect with a narrower optical gate, a higher SNR can be obtained in a homodyne detected signal.

We measured the optical gate waveform by using a CW laser and an electrical sampling oscilloscope with a bandwidth of 65 GHz. This is shown in Fig. 11(a). Figures 11(b) and 11(c) show the waveforms of the electrical modulation signal and detected output signal from the optical gate, and their corresponding FWHMs are 30 ps and 33 ps, respectively. By using the optical gate, the number of tributaries coupled to the coherent receiver was reduced by one third (- 5 dB).

Optics EXPRESS

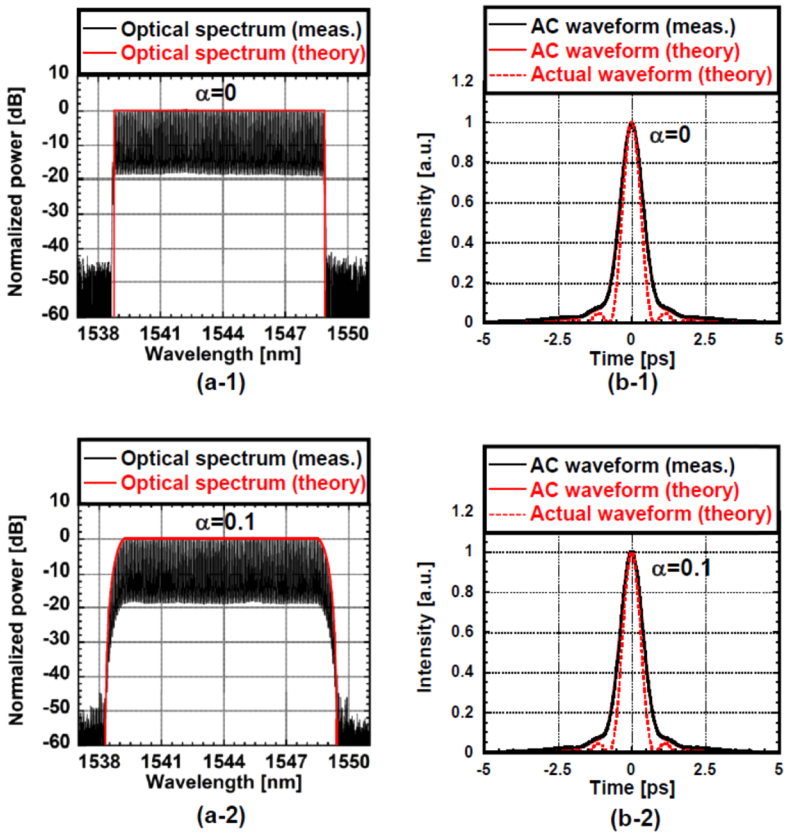

Fig. 9. (a-1) and (a-2) Optical spectra and (b-1) and (b-2) autocorrelation waveforms of the generated Nyquist LO pulse with $\alpha = 0$ and 0.1, respectively.

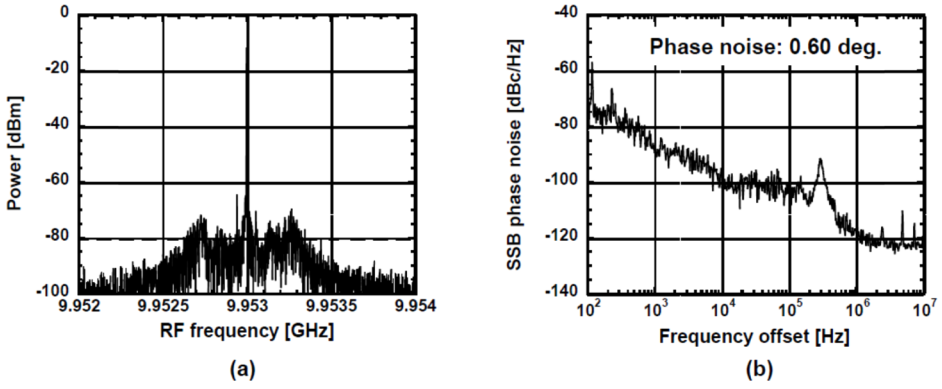

Fig. 10. (a) RF spectrum and (b) SSB phase noise power density of IF signal in OPLL circuit. The transmission distance was 150 km.

Optics EXPRESS

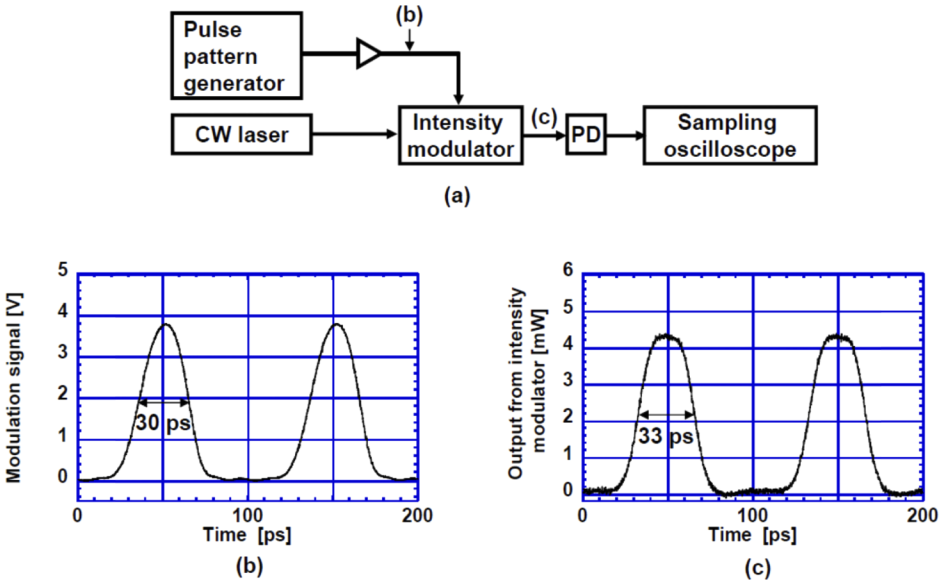

Fig. 11. (a) Measurement setup for optical gate waveform with intensity modulator. (b) (c) Waveforms of electrical modulation signal and detected output signal from optical gate.

We measured the residual self-beat noise without and with the optical gate. The setup is shown in Fig. 12(a), where the Nyquist LO pulse is not coupled and only the OTDM signal is coupled to a coherent receiver. We adjusted the OTDM signal powers to keep the test tributary power the same in both cases. The RF spectra obtained without and with the optical gate are shown in Fig. 12(b) with black and red curves, respectively. We found that the spectrum power from DC to 10 GHz was reduced by 5 dB with an optical gate.

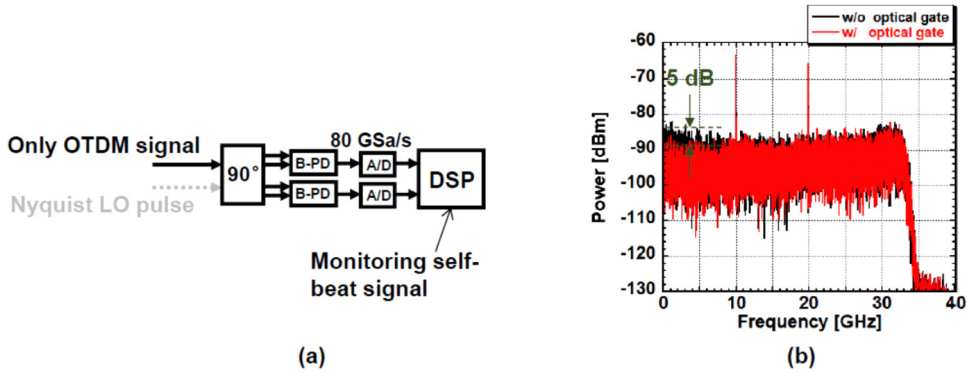

Fig. 12. (a) Measurement setup of residual self-beat signal in balanced PD. (b) RF spectra of self-beat signal (black) without and (red) with optical gate.

Next, we evaluated the demodulation performances without and with an optical gate for a back-to-back condition, where the corresponding constellations are shown in Figs. 13(a) and 13(b), respectively. Without the optical gate, a pattern dependent distortion appeared that was caused by the self-beat noise. In contrast, the distortion was successfully reduced with the optical gate in Fig. 13(b). As a result, the BER was improved from 6.5×10^{-4} to 8.1×10^{-5} by employing the optical gate.

Optics EXPRESS

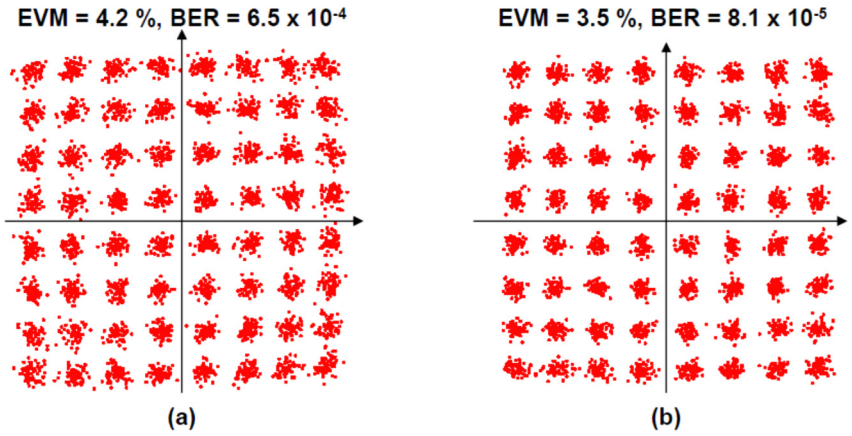

Fig. 13. Constellations of 1.28 Tbaud, 64 QAM signal under a back-to-back condition (a) without an optical gate and (b)with an optical gate.

2.5. Precise timing stabilization between OTDM signal and Nyquist LO pulse

In a high baud rate transmission, very precise timing control is required between the OTDM signal and the Nyquist LO pulse. We controlled the optical path difference between the OTDM signal and the Nyquist LO pulse by using a PLL circuit [12]. In the PLL circuit, the phase difference between a 10 GHz clock extracted from the gated OTDM signal and that extracted from the Nyquist LO pulse was fed back to a piezoelectric transducer (PZT) on which a part of the fiber was wound (see dashed-line box (e) in Fig. 1) to control the timing. Figure 14 shows the changes in the timing fluctuation estimated from an error signal. Without stabilization, drift is observed on a scale of one symbol period within ten minutes. With stabilization, the drift was controlled to within 70 fs, which enabled us to realize precise operation with long-term stability for homodyne detection.

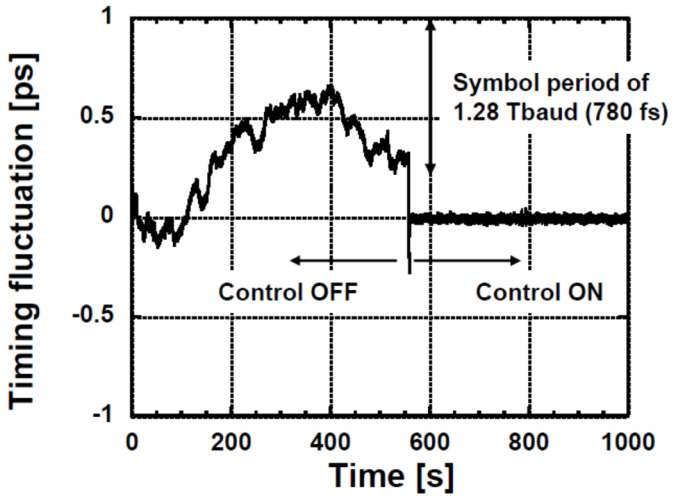

Fig. 14. Change in clock timing between a 1.28 Tbaud OTDM signal and a Nyquist LO pulse before and after control.

Optics EXPRESS

3. Experimental results and their evaluation for 15.3 Tbit/s-150 km coherent Nyquist pulse transmission

We first measured the BER performance of a 15.3 Tbit/s OTDM signal after a 150 km transmission as a function of the fiber launched power. The BER performance is shown in Fig. 15. From this result, the launched power was set at 5 dBm, which was optimally chosen to maximize the OSNR and minimize the nonlinear impairments.

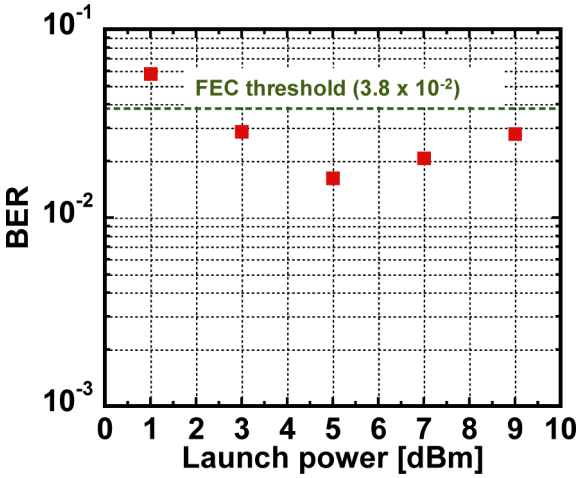

Fig. 15. BER characteristics for one tributary of a 15.3 Tbit/s-150 km signal as a function of the launched power.

Next, we measured the BER performance of a 15.3 Tbit/s signal for different transmission distances. Figure 16 shows the relationship between the BER and the received power measured for one tributary after 75 km and 150 km transmissions. Here, the received power is defined as P_{rec} in Fig. 1. BERs below the forward-error correction (FEC) threshold of 3.8×10^{-2} with an overhead of 25.5% [13] were obtained at received powers of - 20 dBm and - 16 dBm after 75 km and 150 km transmissions, respectively. In each transmission, the BER curves had error floors at 6×10^{-3} and 1.6×10^{-2}, respectively. The BER was increased by 1.0×10^{-2} as the transmission distance was extended from 75 km to 150 km. Figures 17(a) and 17(b) show the constellations of a demultiplexed 10 Gbaud 64 QAM signal after 75 km and 150 km transmissions, respectively. Compared with the back-to-back condition shown in Fig. 13(b), the error vector magnitude (EVM) of the demodulated signal was degraded from 3.5% to 5.8% at 75 km and to 6.7% at 150 km.

The estimated OSNR after a 150 km transmission was 21.5 dB as mentioned in section 2.2. The theoretical BER value for 64 QAM at the OSNR corresponds to 1.5×10^{-3}. On the other hand, the measured BER after a 150 km transmission was 1.6×10^{-2}, which is one order of magnitude larger than that estimated from the OSNR. This indicates that the BER degradation also had other causes including polarization crosstalk, nonlinear impairment, and the bandwidth limitation of the coherent receiver as we describe below.

As regards the polarization crosstalk, we evaluated the BER degradation by comparing the BER performance of single-polarization and polarization-multiplexed transmission. The launched powers were set at - 8 dBm/pol to obtain the same OSNR after a 150 km transmission in both cases. Figure 18 shows the BER performances as a function of the received power in one tributary. The BER curves for a single-polarization and a polarization-multiplexed transmission had error floors at 1.2×10^{-2} and 1.6×10^{-2}, respectively, where the difference between the two BER curves was 0.4×10^{-2}. This was due to a penalty caused by the polarization crosstalk and

Optics EXPRESS

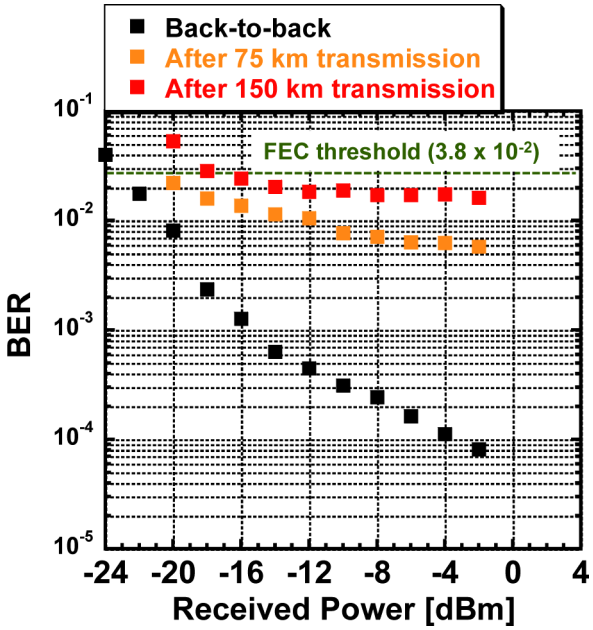

Fig. 16. BER characteristics for one tributary of a 15.3 Tbit/s OTDM signal.

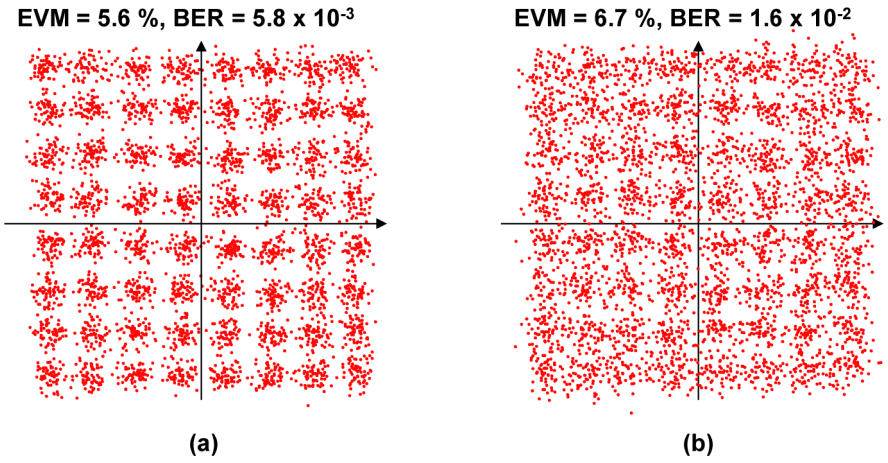

Fig. 17. Constellations of a 1.28 Tbaud, 64 QAM signal after (a) 75 km and (b) 150 km transmissions.

Optics EXPRESS

the cross-phase modulation (XPM) between two orthogonal polarization channels. Compared with the penalty caused by extending the transmission distance (see Fig. 16), the penalty in the polarization-multiplexed transmission was rather small. A large error floor can be seen in the BER characteristics in Fig. 16. This may be attributed to the guided acoustic-wave Brillouin scattering (GAWBS) noise that we reported recently [14]. The error floor may be reduced by compensating for this nonlinear impairment [15].

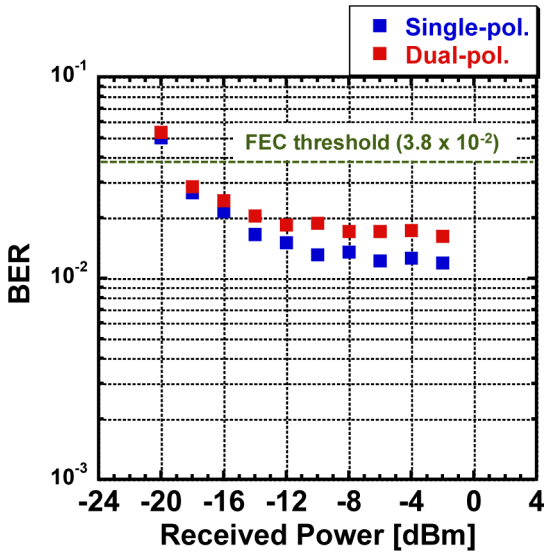

Fig. 18. Comparison of the BER characteristics of single-polarization and polarization-multiplexed transmissions over 150 km.

The bandwidth limitation of the coherent receiver is another factor contributing to the BER degradation. In the present system, the detection bandwidth of the coherent receiver was limited to 33 GHz due to the electrical bandwidth of the digital oscilloscope, which was much narrower than the optical bandwidth of the gated 1.28 Tbaud OTDM signal. The bandwidth limitation reduces the SNR of the electrical signal obtained with homodyne detection.

Finally, we measured the BER for all 128 tributaries in a polarization-multiplexed transmission. The results are shown in Fig. 19. As seen in this figure, a BER below the FEC threshold of 3.8×10^{-2} (25.5% overhead) was successfully achieved for all tributaries. Therefore, a 15.3 Tbit/s signal was successfully transmitted over 150 km in a signal bandwidth of 1.47 THz, which includes 1.41 THz for the OTDM signal and 0.06 THz for the LD and tone signals. This indicates that the SE reached 8.3 bit/s/Hz with a code rate of 0.8 (25.5% overhead).

In the present experiment, the launched power was 5 dBm, which was the same as that used in the 640 Gbaud transmission. This means that the signal power for one tributary was reduced by 3 dB, resulting OSNR degradation. To overcome the problem, a wider detection bandwidth for example 100 GHz will be required instead of the present 33 GHz.

Optics EXPRESS

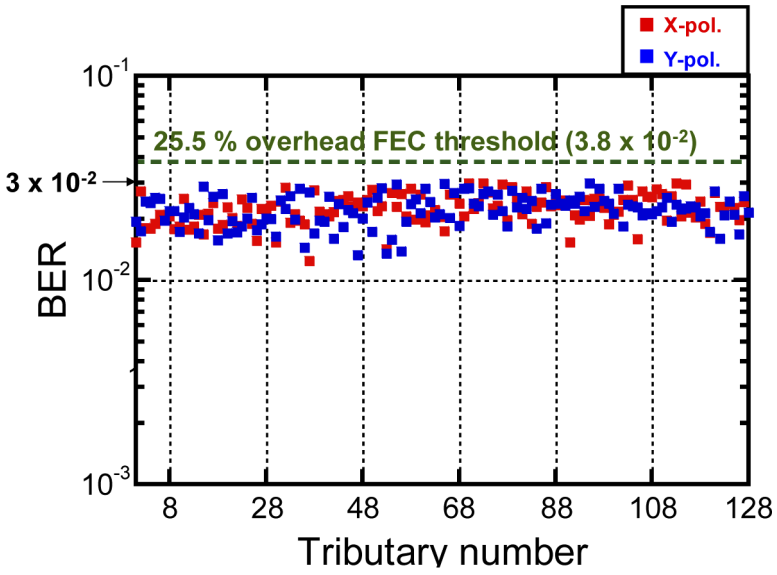

Fig. 19. BERs for all 128 tributaries in a 15.3 Tbit/s-150 km polarization-multiplexed transmission.

4. Conclusions

We successfully demonstrated the first single-channel 15.3 Tbit/s, 64 QAM coherent Nyquist pulse transmission over 150 km, which is the highest speed yet reported for a single-channel transmission. The symbol rate was increased to 1.28 Tbaud using a 670 fs ultrashort coherent Nyquist pulse. We adopted an optical gate and a timing control circuit between the OTDM signal and the Nyquist LO pulse, resulting in a BER below the FEC threshold of 3.8×10^{-2} after a 150 km transmission with an SE of 8.3 bit/s/Hz.

Funding

Japan Society for the Promotion of Science (26000009).

References

1. M. Nakamura, F. Hamaoka, M. Nagatani, Y. Ogiso, H. Wakita, H. Yamazaki, T. Kobayashi, M. Ida, H. Nosaka, and Y. Miyamoto, "192-Gbaud signal generation using ultra-broadband optical frontend module integrated with bandwidth multiplexing function," in *Optical Fiber Communications Conference* 2019, paper Th4B.4.
2. S. Zhalehpour, J. Lin, M. Guo, H. Sepehrian, Z. Zhang, L. Rusch, and W. Shi, "All-silicon IQ modulator for 100 GBaud 32QAM transmissions," in *Optical Fiber Communications Conference* 2019, paper Th4A.5.
3. D. O. Otuya, K. Kasai, T. Hirooka, and M. Nakazawa, "Single-channel 1.92 Tbit/s, 64 QAM coherent Nyquist orthogonal TDM transmission with a spectral efficiency of 10.6 bit/s/Hz," J. Lightwave Technol. **34**(2), 768–775 (2016).
4. J. Nitta, M. Yoshida, K. Kimura, K. Kasai, T. Hirooka, and M. Nakazawa, "Single-channel 3.84 Tbit/s, 64 QAM coherent Nyquist pulse transmission over 150 km with a spectral efficiency of 10.6 bit/s/Hz," Opt. Express **25**(13), 15199–15207 (2017).
5. K. Kimura, J. Nitta, M. Yoshida, K. Kasai, T. Hirooka, and M. Nakazawa, "Single-channel 7.68 Tbit/s, 64 QAM coherent Nyquist pulse transmission over 150 km with a spectral efficiency of 9.7 bit/s/Hz," Opt. Express **26**(13), 17418–17428 (2018).
6. K. Harako, D. O. Otuya, K. Kasai, T. Hirooka, and M. Nakazawa, "High-performance TDM demultiplexing of coherent Nyquist pulses using time-domain orthogonality," Opt. Express **22**(24), 29456–29464 (2014).
7. M. Nakazawa, K. Tamura, H. Kubota, and E. Yoshida, "Coherent degradation in the process of supercontinuum generation in an optical fiber," Opt. Fiber Technol. **4**(2), 215–223 (1998).
8. M. Nakazawa, E. Yoshida, and Y. Kimura, "Ultrastable harmonically and regeneratively modelocked polarization-maintaining erbium-doped fiber ring laser," Electron. Lett. **30**(19), 1603–1605 (1994).

Optics EXPRESS

9. M. Yoshida, K. Kasai, and M. Nakazawa, "Mode-hop-free, optical frequency tunable 40-GHz mode-locked fiber laser," IEEE J. Quantum Electron. **43**(8), 704–708 (2007).
10. M. Yoshida, K. Yoshida, K. Kasai, and M. Nakazawa, "1.55 μm hydrogen cyanide optical frequency-stabilized and 10 GHz repetition-rate-stabilized mode-locked fiber laser," Opt. Express **24**(21), 24287–24296 (2016).
11. C. Boerner, C. Schubert, C. Schmidt, E. Hilliger, V. Marembert, J. Berger, S. Ferber, E. Dietrich, R. Ludwig, B. Schmauss, and H. G. Weber, "160 Gbit/s clock recovery with electro-optical PLL using a bidirectionally operated electroabsorption modulator as phase comparator," Electron. Lett. **39**(14), 1071–1073 (2003).
12. T. Hirooka, R. Hirata, J. Wang, M. Yoshida, and M. Nakazawa, "Single-channel 10.2 Tbit/s (2.56 Tbaud) optical Nyquist pulse transmission over 300 km," Opt. Express **26**(21), 27221–27236 (2018).
13. K. Sugihara, Y. Miyata, T. Sugihara, K. Kubo, H. Yoshida, W. Matsumoto, and T. Mizuochi, "A spatially coupled type LDPC code with an NCG of 12 dB for optical transmission beyond 100 Gb/s," in *Optical Fiber Communication Conference* 2013, paper OM2B.4.
14. M. Nakazawa, M. Yoshida, M. Terayama, S. Okamoto, K. Kasai, and T. Hirooka, "Observation of guided acoustic-wave Brillouin scattering noise and its compensation in digital coherent optical fiber transmission," Opt. Express **26**(7), 9165–9181 (2018).
15. M. Yoshida, N. Takefushi, M. Terayama, K. Kasai, T. Hirooka, and M. Nakazawa, "Reverse phase modulation technique for GAWBS noise error floor elimination in 1024 QAM-160 km digital coherent transmission," in *OptoElectronics and Communications Conference* 2018, paper 4B1-3.